

# Soft Matter

Accepted Manuscript



This is an *Accepted Manuscript*, which has been through the Royal Society of Chemistry peer review process and has been accepted for publication.

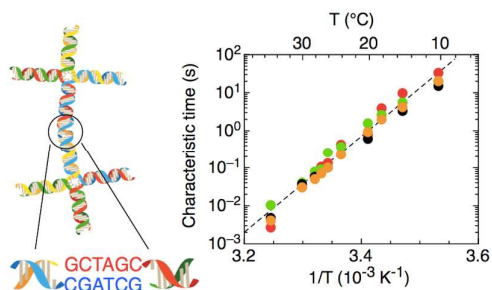
*Accepted Manuscripts* are published online shortly after acceptance, before technical editing, formatting and proof reading. Using this free service, authors can make their results available to the community, in citable form, before we publish the edited article. We will replace this *Accepted Manuscript* with the edited and formatted *Advance Article* as soon as it is available.

You can find more information about *Accepted Manuscripts* in the [Information for Authors](#).

Please note that technical editing may introduce minor changes to the text and/or graphics, which may alter content. The journal's standard [Terms & Conditions](#) and the [Ethical guidelines](#) still apply. In no event shall the Royal Society of Chemistry be held responsible for any errors or omissions in this *Accepted Manuscript* or any consequences arising from the use of any information it contains.

## Equilibrium gels of low-valence DNA nanostars: a colloidal model for strong glass formers

by Silvia Biffi, Roberto Cerbino, Giovanni Nava, Francesca Bomboi, Francesco Sciortino, and Tommaso Bellini



DNA-made colloids of low valence undergo strong-glass type transition with Arrhenius kinetic arrest

# Equilibrium gels of low-valence DNA nanostars: a colloidal model for strong glass formers

Silvia Biffi,<sup>1,2</sup> Roberto Cerbino,<sup>1</sup> Giovanni Nava,<sup>1</sup> Francesca  
Bomboi,<sup>2</sup> Francesco Sciortino,<sup>2,3</sup> and Tommaso Bellini<sup>1</sup>

<sup>1</sup>*Department of Medical Biotechnology and Translational Medicine,  
Università degli Studi di Milano, via Fratelli Cervi 93, I-20090 Segrate (MI), Italy*

<sup>2</sup>*Department of Physics, Sapienza, Università di Roma,  
Piazzale Aldo Moro 2, I-00185, Roma, Italy*

<sup>3</sup>*CNR-ISC, UdR Sapienza, Piazzale Aldo Moro 2, 00185 Rome, Italy*

Kinetic arrest in colloidal dispersions with *isotropic* attractive interactions usually occurs through the destabilization of the homogeneous phase and the formation of a *non-equilibrium* network of jammed particles. Theory and simulations predict that a different route to gelation should become available when the valence of each colloidal particle is suitably reduced. In this condition, gelation should be achievable through a *reversible* sequence of *equilibrium* states. Here we report the reversible dynamic arrest of a dispersion of DNA-based nanoparticles with *anisotropic* interactions and a coordination number equal to four. As the temperature is decreased, the relaxation time for density fluctuations slows down by about five orders of magnitude, following an Arrhenius scaling in the entire experimentally accessible temperature window. The system is in thermodynamic *equilibrium* at all temperatures. Gelation in our system mimics the dynamic arrest of networking atomic strong glass formers such as silica, for which it could thus provide a suitable colloidal model.

Colloidal dispersions have played a crucial role in understanding fundamental problems in condensed matter physics. In particular, extended and continuous efforts have been devoted to the study of the slowing down of the dynamics on approaching the glass and the gel transition. Colloids dominated by repulsive, excluded volume interactions, freeze into non-ergodic states at large concentrations, providing a colloidal counterpart of fragile glass-forming atomic and molecular liquids [1]. Much harder is to devise colloidal models of liquids forming the so-called “strong glass” state [2]. Materials belonging to this class, whose archetype is silica, are characterized by atoms or molecules forming networks with low coordination number and by an Arrhenius slowing down of internal modes with temperature. Deformable repulsive spherical colloids, found to display an Arrhenius dynamics in concentration [3] miss most of the relevant features of these molecular systems: network, attractive interactions, Arrhenius temperature dependence.

Colloids interacting via short-range attractive potential (e.g. depletion) can undergo kinetic arrest entering a state in which the particles form an extended network [4, 5], generally referred to as a *gel* state. In the case of spherical particles, and more in general of particles whose attractive interaction is isotropic, colloidal gels are produced upon quenching the dispersion into the unstable region, across the liquid-gas-like phase boundary [5–9]. During the phase separation following the quench, colloids condense into a interconnected network of locally dense glassy regions. The system eventually freezes into a disordered heterogeneous gel which retains the structural pattern imposed by the interrupted spinodal decomposition [8]. Despite their network structure, this route to gelation has little in common with network-forming atomic glasses since the dynamic arrest is here obtained through a discontinuous transition to a non-equilibrium state and since the jamming is provided by the tight packing and large coordination number of the interacting particles.

Phase-separation mediated gelation is however only one of the mechanisms expected to generate a colloidal gel. Recent numerical and theoretical studies [10, 11] have suggested the possibility of a different route available when colloidal particles can interact with a limited number of neighbours only. In this condition the liquid-gas unstable region shrinks toward lower concentrations and an interval of moderate concentrations ( $c$ ) becomes available in which the temperature can be lowered without incurring in phase separation [10–12]. Cooling in this range of  $c$ , where the only arresting mechanism is the increasingly large lifetime of inter-particle bonds, is expected to lead to a kinetically-arrested homogeneous

gel through a continuum of equilibrium states with intermediate dynamical response [12]. This path toward gelation, controlled by the bond lifetime rather than by excluded volume interactions, is analogous to the dynamic arrest that characterizes “strong” network glass formers [13], molecular system for which they could provide the colloidal counterpart.

Although various strategies for synthesizing colloidal particles with specific valence have been developed in the last years [14–16], the production protocol of these patchy particles is far from yielding the bulk quantities that would be necessary to explore their collective thermodynamic and dynamic behavior. An alternative approach for the production of limited valence particles exploits the remarkable effectiveness of DNA self-assembly in the fabrication of nanostructures [17–19]. This strategy enables the production of large amounts of identical nanoparticles with controlled valence and interaction strength [20–23], suitable for the investigation of the phase behavior [23].

In this article we report the first experimental study of the dynamical changes accompanying equilibrium gelation in a system of well-defined valence DNA-nano-stars (NS), whose phase-diagram was previously determined in Ref. [23]. To this aim we selected concentrations large enough not to incur in the liquid-gas phase separation. At such concentrations, if no other phase transition occurs, the system is expected to be homogeneous and stable at all temperatures ( $T$ ) down to water freezing. Our data confirm that these systems evolve from a homogeneous “fluid” state of free NS in solution at high  $T$ , to a homogeneous dynamically arrested, highly viscous state at low  $T$ , where a macroscopically extended network of strongly bound NS is formed. Such transition is found to be continuous, with the “fluid” of DNA-NS progressively slowing down toward a dynamically arrested gel through a reversible sequence of equilibrium states.

## Results

### DNA nanostars.

Low valence colloids are obtained via self-assembly of DNA single strands of suitably chosen sequences (see Methods) at temperatures lower than  $\approx 65^\circ\text{C}$ . Each particle results from the aggregation of four distinct strands and takes the shape of a NS with four arms (of length  $\ell \approx 8 \text{ nm}$ ) terminating with identical overhanging unpaired sequences that provide the NS-NS interaction (Fig. 1-a). The overhangs, which become sticky for temperatures lower than  $\approx 40^\circ\text{C}$ , are made of 6-base long self-complementary single strands (*CGATCG*).

Unpaired bases are inserted by sequence design just before the overhang sticky sequence as well as in the particle core, so that the angle between the arms of a NS can fluctuate, their relative distance being controlled mainly by steric and electrostatic repulsion. Previous combined experiments of optical microscopy, UV absorbance and light scattering, devoted to determine the phase behavior of this system [23], demonstrated the presence of an unstable region in the  $c-T$  space where the aqueous dispersion separates into a "gas" and a "liquid" of NS. Fig. 1-b shows the binodal line for such a transition, obtained from concentration measurements of coexisting gas and liquid phases. At low  $T$ , the density of the coexisting liquid was found to be  $c_l \approx 17 \pm 1$  mg/ml. In line with theoretical predictions [11],  $c_l$  is comparable to the minimum density of fully bonded networks, in which each particle is surrounded by four neighbours. Such a density is much smaller than the one of a "liquid" of isotropically interacting colloids, whose number of neighbours is typically much larger ( $\approx 12$ ). Concentrations  $c \gtrsim c_l$ , where no phase separation takes place on cooling can be accessed experimentally without incurring neither into experimental issues such as large viscosity or mis-shaped structures, nor into packing limitations, making DNA NS an ideal system to explore the features of reversible equilibrium gelation. To investigate equilibrium gelation we thus prepared samples at two DNA NS concentrations,  $c_1 \approx 17.5$  mg/ml ( $\geq c_l$ ) and  $c_2 \approx 21.3$  mg/ml ( $> c_l$ ) and studied their behavior as a function of temperature. Sample preparation procedure (see Methods) ensures that the  $c_1$  sample does not cross the phase boundary in the explored range. Inspection of samples by optical microscopy confirms that they remain homogeneous and clear, with no sign of phase separation, in the whole  $T$  range.

As observed in investigating colloids with DNA-mediated attractive interactions [24], inter-particle interactions provided by DNA pairing are particularly convenient to investigate gelation because of the large entropic component of the hybridization free energy, which makes the inter-particle interactions strongly  $T$  dependent. This can be appreciated by inspecting the right axis of Fig. 1-b, reposting the ratio between the bonding free energy  $\Delta G_{nn} = -44.6 + 0.13T$  kcal/mol involved in each overhang interaction (as calculated according to the standard nearest-neighbor model [25]) and the thermal energy  $RT$  (where  $R$  is the gas constant). In the temperature range of  $35^\circ\text{C}$  examined in this work, the ratio increases by over a factor of two. Such a large span of  $\Delta G_{nn}/RT$  cannot be obtained with more conventional particles where the attractive interaction has a weaker dependence on  $T$ .

**Light scattering.**

To investigate the homogeneity of the samples on mesoscopic length-scales, we measured the dependence of the scattered intensity  $I(q, T)$  on wave-vector  $q$  and  $T$ . The small sample volumes employed in this study ( $\approx 50 \mu\text{l}$ ) make it hard to precisely evaluate the effective scattering volume, given by the overlap between the illuminating beam, the collected modes and the actual cell. Therefore, while the determination of  $q$  itself and the dynamics are accurate, we have less precision in the measurement of the  $q$  dependence of the scattered intensity. Within our experimental accuracy, no significant  $q$  dependence was observed (see Fig. 2 of ESI), indicating that at the  $q$  values accessible by light scattering ( $q \ll 2\pi/\ell$ ) the system remains nearly homogeneous at all the explored  $T$ . Such behavior marks a substantial difference with the one observed in the critical system, where concentration fluctuations develop on the mesoscale (see Ref. [23] and Fig.2 of ESI).

Fig. 2-a shows  $I(T)$  measured along the thermodynamic paths indicated by the two vertical lines in Fig. 1-b (continuous at  $c_1$  and dashed at  $c_2$ ). In both systems,  $I(T)$  exhibits a mild increase on cooling, but no sign of incurring in spinodal instability or a critical point which would lead to a singular behavior such as the one found along the critical isochore (dotted line in Fig. 1-b) in Ref. [23], here reported for comparison (diamonds in Fig. 2). The fact that the growth of  $I(T)$  observed upon lowering  $T$  in the  $c_1$  sample is larger than the one of the  $c_2$  sample may reflect its closer proximity to the binodal line.

Dynamic light scattering measurements performed along the same paths reveal instead a strong change in the kinetic behavior. Fig. 1-c shows a selection of the collective intermediate scattering functions  $g_1(\tau)$  measured at various  $T$  for  $c_1$  (analogous results can be found for  $c_2$  in the ESI). While at high  $T$  a single process dominates the dynamics, upon cooling a two-step relaxation develops, the slower process undergoing a very marked and progressive slowing down.

As previously proposed for gels [26, 27], we quantify the collective dynamics of the system by representing  $g_1(\tau)$  as a sum of an exponential and of a stretched exponential decay,

$$g_1(\tau) = (1 - A_s)e^{-\frac{\tau}{\tau_f}} + A_s e^{-(\frac{\tau}{\tau_s})^{\beta_s}} \quad (1)$$

modeling the fast ( $f$ ) approach to the plateau  $A_s$  and the slow ( $s$ ) relaxation to zero, respectively. This functional form is also commonly used to interpret the decay of correlations in systems approaching dynamic arrest [13], including transient networks [28]. For all  $T$  and all  $q$  the functional form in Eq. 1 provides a quite accurate description of the decay of

the density fluctuations, as can be seen in Fig. 1-c. Since the stretching exponent  $\beta_s$  was found to consistently assume values between 0.6 and 0.7, we fixed it to  $\beta_s = 0.7$  to provide a uniform analysis to all the relaxation curves.

### Testing thermodynamic equilibrium

Given the relevance of determining whether the DNA-NS system is in thermodynamic equilibrium in all the explored  $T$  range, we carefully examined this aspect. An important indicator is offered by the relative mean squared intensity fluctuation  $r = \langle I^2 \rangle / \langle I \rangle^2$ , obtained from the ratio of the  $\tau = 0$  and at  $\tau = \infty$  values of the correlation function of the scattered intensity. A typical effect of the loss of ergodicity is the decrease of such a ratio and its dependence on the specific position where the scattered intensity is collected, which indicates a growing static component in the scattered intensity. Here instead,  $r$  does not decrease with decreasing  $T$  and it remains constant upon rotating the sample in the light scattering apparatus. This evidence supports the notion that for  $t > \tau_s$  all fluctuations in  $c$  are fully relaxed, which is by itself a clear indication of ergodicity in the length scales probed by light scattering.

To further strengthen this conclusion, and rule out the presence of possible metastable states, we thermally cycled between 10 and 45°C one of the samples at  $c_1$  along various  $T$  paths. Measurements at two target  $T$  (15 and 20°C) were taken both by slowly ramping  $T$  (by about 1 °C/hour) and after fast quenches (of about 1 °C/min). The results are shown in Fig. 3, where we represent the  $g_1(\tau)$  measured after various thermal paths (panel a) together with the corresponding fitting parameters (panel b). Within our experimental accuracy we could not detect any dependence of the thermalized states on their previous conditions. We thus conclude that along the explored path our data always refer to equilibrium fluid states.

### Approach to gelation

The  $T$  and  $q$  dependences of the fit parameters are shown in Fig. 4-a and in Fig. 5 for both  $c_1$  and  $c_2$ . The characteristic time of the fast decay,  $\tau_f$  (4-a, full dots), is very weakly dependent on  $T$  while it shows an appreciable dependence on  $q$ . Fig. 5-a shows that  $\tau_f$  data are compatible with a  $q^{-2}$  dependence. By contrast, the characteristic time of the slow relaxation,  $\tau_s$  (empty dots), is found to be  $q$  independent, as shown in Fig. 5-b. Both  $\tau_f$  and  $\tau_s$  are nearly identical for  $c_1$  and  $c_2$ , indicating that the dynamic behavior of these gelling systems do not depend significantly on  $c$ .

The  $T$  dependence of  $\tau_s$ , shown in Fig. 4-a, is characterized by a neat activated-type

behavior, as evident by the agreement between data and the dashed line, representing the best fitting Arrhenius equation  $\tau_s = \tau_0 \exp(\Delta G(T)/RT)$ , where  $\Delta G(T)$  is the variation of Gibbs free energy involved in the activation process and  $\tau_0$  is the high  $T$  limit of  $\tau_s$ . We previously found an analogous Arrhenius slowing down in a more restricted  $T$  range studying samples prepared at the critical concentration [23]. In that case, only  $T > 25$  °C could be investigated before entering the coexistence region, a constraint that forbade exploring gelation in the absence of phase separations. Here instead, samples can be cooled down to freezing without phase-separating. At both concentrations  $c_1$  and  $c_2$ , the system is characterized by a growth of  $\tau_s$  of more than 5 orders of magnitude, from  $100\mu\text{s}$  to over  $10\text{s}$ , marking an impressive dynamic arrest under equilibrium conditions. Such kinetic behavior coherently combines with the data in Fig. 2 to indicate that in the whole range up to gelation the system smoothly evolves with no structural or dynamical singularity. The independence of the relaxation time on  $c$  strongly suggests that temperature, as opposed to concentration, controls the relaxation time, generating in the equilibrium  $T - c$  gel phase isochrones parallel to the concentration axis [12]. Fig. 4-a displays  $\ln(\tau_s)$  vs.  $(RT)^{-1}$  so to enable extracting  $\Delta H$  from the slope, while the intercept contains combined information on  $\tau_0$  and  $\Delta S$ . From the simultaneous fit of data at different  $q$  we find  $\Delta H \approx 58 \pm 5$  kcal/mol. Such value indicates that the free energy barrier of the activated relaxation process is comparable with the enthalpy of 1.3 overhang bonds as estimated by the nearest-neighbour model [25]. Assuming  $\Delta S = 170$  cal/mol/K, the value of Ref. [25] for 1.3 bonds, it is possible to estimate the attempt time  $\tau_0$  from the intercept of the line  $\ln(\tau_s)$  vs  $(RT)^{-1}$ , obtaining  $\tau_0 \approx 1\mu\text{s}$ . The estimate of 1.3 bonds has some factors of uncertainty, including the differences in hybridization enthalpy when computed according to the various values of the thermodynamic parameters found in literature [19], the stabilizing effect of the presence of bases adjacent to the paired 6-mer [25], and the destabilizing effects of long DNA sequences connected to a paired ones [29]. While all these factors make it impossible obtaining a secure determination of the activation energy as a multiple of the single inter-NS bond enthalpy, the data unambiguously indicate that the activation energy is of the same order of such DNA-DNA bonds.

These results suggest that once the network is formed, the system dynamics is enslaved to the activated elementary step of bond-breaking. Why is the energy involved in the network rearrangement approximately 1.3 bonds and not a larger value compatible with the average

binding energy of each DNA-NS remains, at this stage, an open issue. In part this could be due to the larger probability of unhooking from the network of DNA-NS with a reduced number of bonds. Answering this question would imply developing a rather detailed model of the dynamics of transient networks.

The notion of kinetic arrest through the progressive formation of an extended network of bound DNA-NS is supported by the behavior of the viscosity of the system, the other typical quantifier of the dynamical arrest, which we could measure in the case of the  $c_1$  system (see ESI). Indeed, we find that the viscosity depends on  $T$  through an Arrhenius behavior with equal  $\Delta H$ . The approach to kinetic arrest through an equal Arrhenius law in both relaxation rate of spontaneous fluctuations and in viscosity is indeed the defining property of strong glass formers [13], compounds typically having a limited coordination number and forming arrested phases at reduced densities lower than the fragile glass formers. All these features are captured by the DNA-NS system here investigated.

The observed  $q$ -independence of  $\tau_s$  and  $q^{-2}$  dependence of  $\tau_f$  are features that are remarkably shared by other physical gels [28]. The  $q$ -independence of  $\tau_s$  suggests that the network rearrangements that follow bond breaking events equally contributing to all length scales probed in our experiments. This feature could be produced by relaxations that act over distances much larger than the nearest neighbour distances. The  $q^{-2}$  dependence of  $\tau_f$  indicates a diffusive process that maintains the same time scale across the explored temperature window, over which the system moves from a collection of freely diffusing nanostars (or small aggregates) to a fully bonded network where all particles are connected in the same cluster. Consistently,  $\tau_f$  quantifies how the collective density fluctuations decay over length scales significantly larger than the nearest neighbour distance due to the free diffusion of small aggregates at high  $T$  and to the diffusive density fluctuations of the constrained network structure at low  $T$ . This latter behavior could be analogous to the concentration fluctuations in polymer gels due to mesh fluctuations.

### Non-ergodicity factor

The activated slowing down observed here is the consequence of the remarkably long lifetime of oligomer DNA duplexes and of its dramatic  $T$  dependence [30], features that already enabled unveiling unexpected self-assembly processes otherwise hard to detect [31]. If the bond lifetime were infinite as in chemical gels, the network would not restructure and the long time limit of  $g_1(\tau)$  would coincide with  $A_s$  [32, 33]. Here instead the non-ergodic

behavior is resolved by the activated unbinding of the NS overhangs, which reestablishes the access to the whole conformational space for  $\tau > \tau_s$ . The two-step behavior of the correlation function is characteristic of systems continuously approaching a kinetic arrested state and it is also commonly observed in supercooled glass-forming liquids. However, differently from the glass case, where the plateau height remains constant — suggestive of a localization length that does not change on supercooling until the (ideal) glass transition is reached [34] — here we observe a clear growth of the plateau height (commonly indicated in the glass community as *non-ergodicity factor* [13]), correlated with the slowing down of the dynamics.

As it can be appreciated from Fig. 4-b, the non ergodicity factor  $A_s$  significantly grows with cooling, progressively increasing from zero at high  $T$ , where NS are not interacting, up to  $\approx 0.9$  (for  $c_1$ ) and  $\approx 0.8$  (for  $c_2$ ) at the lowest investigated  $T$ . The amplitude of  $A_s$  does not depend on  $q$  in the explored hydrodynamic region. Previous theoretical [35] and numerical [32, 36, 37] studies of the self-dynamics in chemical gels (infinite bond lifetime) have associated the emergence of non-ergodicity to the percolation transition, with the non-ergodic component of  $g_1(\tau)$  continuously growing with the fraction of particles frozen in the infinite spanning clusters. In analogy, we interpret the growth of  $A_s$  in our collective intermediate scattering functions as a consequence of the network consolidation caused by the progressive attachment of the NS to the percolating aggregate. Fig. 4-b displays the fraction  $f$  of paired overhangs as a function of  $T$ , as calculated by following Ref. [38], which indeed traces the growth of  $A_s$  in the entire  $T$  window. The smaller value of  $A_s$  observed at  $c_2$  may indeed indicate that at concentrations above the one of ideal crystal, at which  $f = 1$ , the fraction of bound overhangs decreases with  $c$ . This appears reasonable given the large space available within the 3D NS network, that can easily accommodate intercalating branches of NS.

The fortunate combination of bond strength and lifetime enables to observe and characterize the two step relaxation already starting from low values of  $A_s$ , approximately corresponding to  $f \approx 1/3$ , the mean-field estimate for the fraction of formed bonds yielding percolation in a system of particles with valence four [39].

## Conclusions

By exploiting the programmability of the interactions among DNA nanostars, we have provided the first experimental demonstration of reversible equilibrium gelation in limited va-

lence particles. On lowering  $T$ , the system progressively evolves into a kinetically arrested state through a sequence of equilibrium states characterized by an increasingly slow dynamics without incurring in phase transitions. Both the density relaxation time and the viscosity display an Arrhenius dependence on  $T$ , a behaviour corresponding to the onset of the glass state in network glass-forming liquids [13], providing the first colloidal model for strong glasses. However, differently from this class of atomic and molecular network-former systems, here the non-ergodicity factor crucially depends on  $T$ . We attribute this to the fact that in atomic systems the bond lifetime is so fast that the two-step relaxation becomes detectable only when the network is fully formed. Here instead the inter-NS bonds are already long-lived close to percolation, a condition enabling us to detect the equilibrium pathway toward gelation, inaccessible in ordinary glass-forming liquids.

Our observation of a continuum transition into the gel state by cooling samples having concentrations larger than the instability region, agrees with recent studies on the thermodynamic stability of tetrahedral coordinated particles showing that bond flexibility, certainly present in the DNA-NS system, entropically stabilizes the disordered, fully-bonded structure, rendering the gel more stable than any crystal phase [40, 41]. The experimental evidence of absence of crystallization — despite the investigated sample concentration is the same as the one of a tetrahedral open crystal (diamond) and despite the several months shelf life of our samples — points in this direction.

Overall, our results confirm and extend the relevance of colloids as models for the investigation of the glass state. As hard-sphere colloids were demonstrated to be a paradigmatic system to explore fragile glass formers [42–44], DNA-based directional colloids will possibly contribute to the understanding of the glass transition in strong glasses.

## Methods

**Sample preparation.** DNA NS results from the self-assembly of four 49-base long DNA oligomers. Sequences are as follows:

Sequence 1:

5'-CTACTATGGCGGGTGATAAAAACGGGAAGAGCATGCCCATCCACGATCG-3'

Sequence 2:

5'-GGATGGGCATGCTCTTCCCGAACTCAACTGCCTGGTGATACGACGATCG-3'

Sequence 3:

5'-CGTATCACCAGGCAGTTGAGAACATGCGAGGGTCCAATACCGAC**CGATCG**-3'

Sequence 4:

5'-CGGTATTGGACCCTCGCATGAATTTATCACCCGCCATAGTAGA**CGATCG**-3'

Each strand is designed to bind to two other strands in two 20-nucleotide-long regions (underlined letters), which form the arms of the structure. Each arm ends in a single stranded 6-bases long overhang (bold letters) of sequence CGATCG. Since the sequence of the overhangs is self-complementary, and being it identical in all arms, it provides a sticky-type interaction between the nanostar tips. In-between the arm forming sequences, as well as before the overhang sequence, unpaired A bases have been inserted in order to release angular constraints between the arms. Page purified DNA was purchased by PRIMM srl. Desalting was performed using Illustra NAP-10 columns (GE Healthcare). Samples of valence-4 DNA-NS were prepared at  $c_1 \approx 17.5 \text{ mg/ml}$  and at  $c_2 \approx 21.3 \text{ mg/ml}$ . DNA was hydrated using NaCl electrolyte solutions so to yield a total estimated ionic strength, which also includes the dissociated ions, of  $\approx 50\text{mM}$ . The pH of the resulting solution was measured and found to be in the range 7-8. All samples were heated to  $90^\circ\text{C}$  and slowly cooled to  $30^\circ\text{C}$  in approximatively four hours to allow the formation of the NS. The sample at  $c_1$  was prepared by exploiting phase separation: we initially prepared a dispersion at the critical concentration  $c^* = 9 \text{ mg/ml}$ , cooled it at  $T = 4^\circ\text{C}$  and centrifuged in order to speed up the phase separation process. The vapor phase was then carefully removed and the procedure was iterated until no further phase separation was observed, leaving a dense sample at concentration  $c_1 \approx c_l$ .

**Light scattering.** Static and dynamic light scattering measurements were performed with a customized light scattering setup (Scitech Instruments) equipped with a  $532\text{nm}$  solid-state laser source. Scattered light is collected by an optical fiber carrying few propagation modes, yielding values of  $\langle I^2 \rangle / \langle I \rangle^2 \approx 0.5$ , for ergodic samples. Most of the data were taken at the scattering wave-vector  $q = 22.3 \mu\text{m}^{-1}$  ( $\theta = 90^\circ$ ) as a function of  $T$ , in the range  $10^\circ\text{C} \leq T \leq 45^\circ\text{C}$ . For each  $T$  three sets of acquisition spaced by two hours intervals were run. Additional data, with less statistics, were taken at  $q = 12.1 \mu\text{m}^{-1}$ ,  $q = 17.6 \mu\text{m}^{-1}$ , and  $q = 30.6 \mu\text{m}^{-1}$ . All explored  $q$  are well into the hydrodynamic regime.

## References:

---

- [1] P. N. Pusey and W. Van Megen, *Phys. Rev. Lett.* **59**, 2083 (1987).
- [2] C. A. Angell, *J. Non-Cryst. Solids* **131-133**, 13 (1991).
- [3] J. Mattsson *et al.*, *Nature* **462**, 83 (2009).
- [4] K. N. Pham, A. M. Puertas, J. Bergenholtz, S. U. Egelhaaf, A. Moussaïd, P. N. Pusey, A. B. Schofield, M. E. Cates, M. Fuchs, and W. C. K. Poon, *Science* **296**, 104 (2002).
- [5] W. C. K. Poon, A. D. Pirie, M. D. Haw, and P. N. Pusey, *Physica A* **235**, 110 (1997).
- [6] E. De Hoog, W. Kegel, A. Van Blaaderen, and H. Lekkerkerker, *Phys. Rev. E* **64**, 021407 (2001).
- [7] S. Buzzaccaro, R. Rusconi, and R. Piazza, *Phys. Rev. Lett.* **99**, 098301 (2007).
- [8] P. J. Lu, E. Zaccarelli, F. Ciulla, A. B. Schofield, F. Sciortino, and D. A. Weitz, *Nature* **453**, 499 (2008).
- [9] M. Laurati, G. Petekidis, N. Koumakis, F. Cardinaux, A. B. Schofield, J. M. Brader, M. Fuchs, and S. U. Egelhaaf, *J. Chem. Phys.* **130**, 134907 (2009).
- [10] E. Zaccarelli, S. V. Buldyrev, E. L. Nave, A. J. Moreno, I. Saika-Voivod, F. Sciortino, and P. Tartaglia, *Phys. Rev. Lett.* **94**, 218301 (2005).
- [11] E. Bianchi, J. Largo, P. Tartaglia, E. Zaccarelli, and F. Sciortino, *Phys. Rev. Lett.* **97**, 168301 (2006).
- [12] E. Zaccarelli, *J. Phys. Cond. Mat* **19**, 323101 (2007).
- [13] K. Binder and W. Kob, *Glassy Materials And Disordered Solids: An Introduction to Their Statistical Mechanics* (World Scientific Publishing Company, 2005).
- [14] E. Bianchi, R. Blaak, and C. N. Likos, *Phys. Chem. Chem. Phys.* **13**, 6397 (2011).
- [15] A. B. Pawar and I. Kretzschmar, *Macromol. Rapid Comm.* **31**, 150 (2010).
- [16] S. Jiang, S. Granick, and H.-J. Schneider, *Janus Particle Synthesis, Self-Assembly and Applications* (Royal Society of Chemistry (RSC), 2012).
- [17] N. C. Seeman, *Nature* **421**, 427 (2003).
- [18] N. C. Seeman, *J. Theor. Biol.* **99**, 237 (1982).
- [19] T. Bellini, R. Cerbino, and G. Zanchetta, *Topics in Current Chemistry* **318**, 225 (2012).
- [20] J. B. Lee, S. Peng, D. Yang, Y. H. Roh, H. Funabashi, N. Park, E. J. Rice, L. Chen, R. Long,

- M. Wu, *et al.*, *Nature Nanotechnology* **7**, 816 (2012).
- [21] Y. Li, Y. D. Tseng, S. Y. Kwon, L. d’Espaux, J. S. Bunch, P. L. McEuen, and D. Luo, *Nature Mater.* **3**, 38 (2004).
- [22] Y. H. Roh, R. C. H. Ruiz, S. Peng, J. B. Lee, and D. Luo, *Chem. Soc. Rev.* **40**, 5730 (2011).
- [23] S. Biffi, R. Cerbino, F. Bomboi, E. M. Paraboschi, R. Asselta, F. Sciortino, and T. Bellini, *Proc. Nat. Acad. Sci.* **110**, 15633 (2013).
- [24] R. Dreyfus *et al.*, *Phys. Rev. Lett.* **102**, 048301 (2009).
- [25] J. SantaLucia, *Proc. Natl. Acad. Sci. USA* **95**, 1460 (1998).
- [26] J. Martin, J. Wilcoxon, and J. Odinek, *Phys. Rev. A* **43**, 858 (1991).
- [27] R. Liu, X. Gao, and W. Oppermann, *Polymer* **47**, 8488 (2006).
- [28] E. Michel, M. Filali, G. Aznar, R. Porte, and J. Appell, *Langmuir* **16**, 8702 (2000).
- [29] L. Di Michele *et al.*, *J. Am. Chem. Soc.* **136**, 6538 (2014).
- [30] M. T. Woodside, W. M. Behnke-Parks, K. Larizadeh, K. Travers, D. Herschlag, and S. M. Block, *Proc. Natl. Acad. Sci. U.S.A.* **103**, 6190 (2006).
- [31] T. Bellini, G. Zanchetta, T. Fraccia, R. Cerbino, B. Tsai, G. P. Smith, M. J. Moran, D. M. Walba, and N. A. Clark, *Proc. Natl. Acad. Sci.* **109**, 1110 (2012).
- [32] I. Saika-Voivod, E. Zaccarelli, F. Sciortino, S. V. Buldyrev, and P. Tartaglia, *Phys. Rev. E* **70**, 041401 (2004).
- [33] P. I. Hurtado, L. Berthier, and W. Kob, *Phys. Rev. Lett.* **98**, 135503 (2007).
- [34] W. Götze, in *Liquids, Freezing and Glass Transition*, Les Houches Summer Schools of Theoretical Physics, Vol. Session LI (1989), edited by J. P. Hansen, D. Levesque, and J. Zinn-Justin (North Holland, Amsterdam, 1991) pp. 287–503.
- [35] K. Broderix, H. Löwe, P. Müller, and A. Zippelius, *Phys. Rev. E* **63**, 011510 (2000).
- [36] E. D. Gado, A. Fierro, L. de Arcangelis, and A. Coniglio, *EPL (Europhysics Letters)* **63**, 1 (2003).
- [37] J. Colombo, A. Widmer-Cooper, and E. Del Gado, *Phys. Rev. Lett.* **110**, 198301 (2013).
- [38] J. Zadeh, C. Steenberg, J. Bois, B. Wolfe, M. Pierce, A. Khan, R. Dirks, and N. Pierce, *J. Comput. Chem.* **32**, 170 (2011).
- [39] D. Stauffer and A. Aharony, *Introduction to Percolation Theory*, 2nd ed. (Taylor and Francis, London, 1992).
- [40] F. Smallenburg and F. Sciortino, *Nature Physics* **9**, 554 (2013).

- [41] L. Rovigatti, F. Romano, F. Smalenburg, and F. Sciortino, *ACS nano* **8**, 3567 (2014).
- [42] P. N. Pusey and W. van Meegen, *Nature* **320**, 340 (1986).
- [43] P. N. Pusey and W. van Meegen, *Phys. Rev. Lett.* **59**, 2083 (1987).
- [44] W. Poon, *Science* **304**, 830 (2004).

## **Acknowledgements.**

We acknowledge support from the Italian Ministry of Education and Research, projects PRIN (2010LKE4CC “Building Materials with DNA bricks”) and Futuro in Ricerca (RBFR125H0M). SB, FB and FS also acknowledge support from ERC-226207-PATCHYCOLLOIDS. We thank R. Asselta, F. Bordi, P. Filetici and E.M. Paraboschi for discussions.

## **Additional information**

Electronic Supplementary Information (ESI) available. See DOI: 10.1039/b000000x/

**Competing financial interests:** The authors declare no competing financial interests.

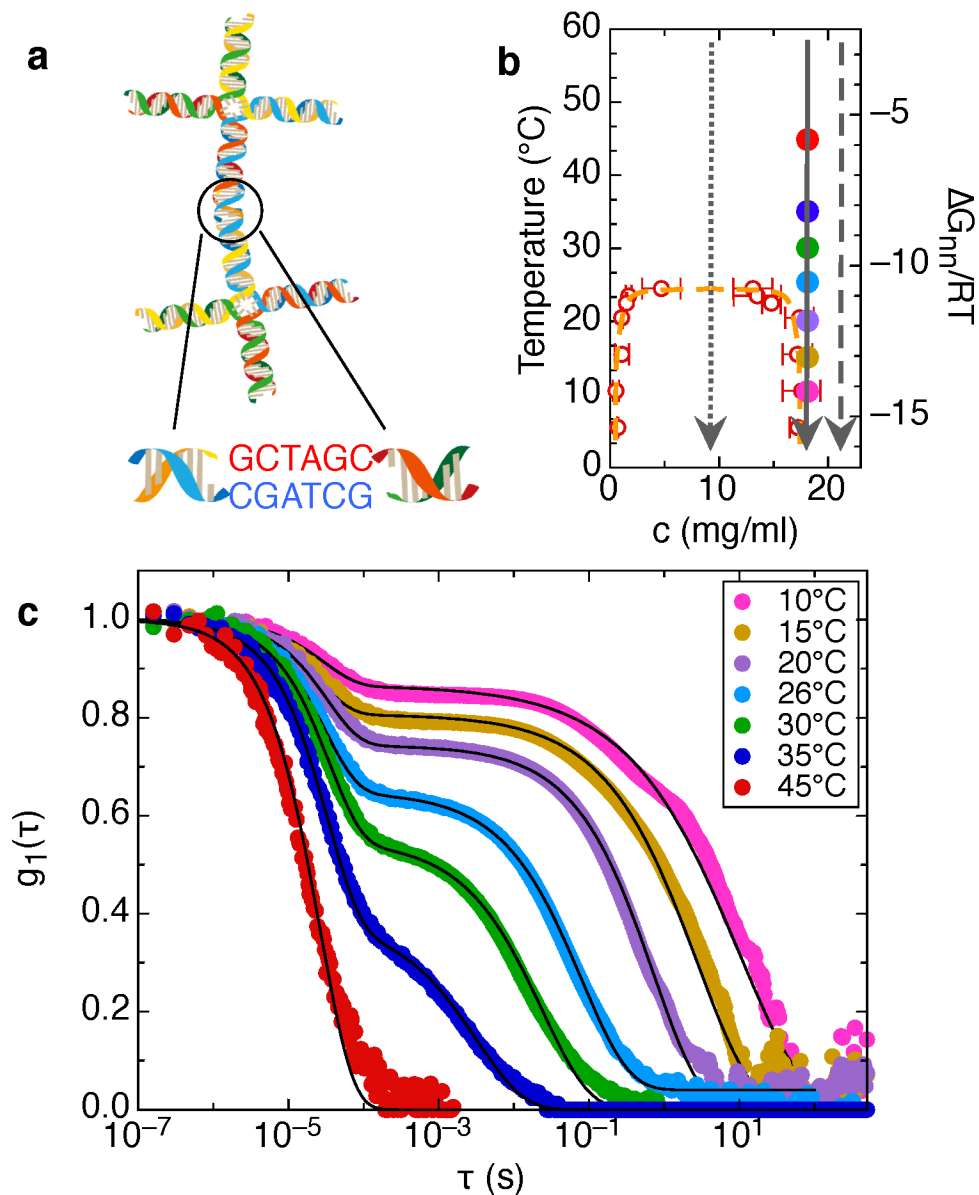


FIG. 1. (a) Pictorial view of a valence-4 DNA NS resulting from the self assembly of four DNA oligomers. Inter-NS interactions are provided by the hybridization of the 6-base-long overhangs on the arm tips. (b) Phase diagram of DNA nano-stars with valence-4 from Ref. [23]. Red symbols and orange dashed line mark the gas-liquid binodal line. The vertical lines indicates the valence-4 NS concentrations explored in this work:  $c_1$  (continuous line),  $c_2$  (dashed line). The dotted line indicates the critical isochore. The colored dots at  $c_1$  the mark temperatures at which the correlation functions in panel C were measured. (c) Intermediate scattering functions  $g_1(\tau)$  vs. time  $\tau$  measured at selected temperatures, as indicated by color matching with panel B, at  $q = 22.3\mu\text{m}^{-1}$ . Lines represent the best fit according to Eq. 1.

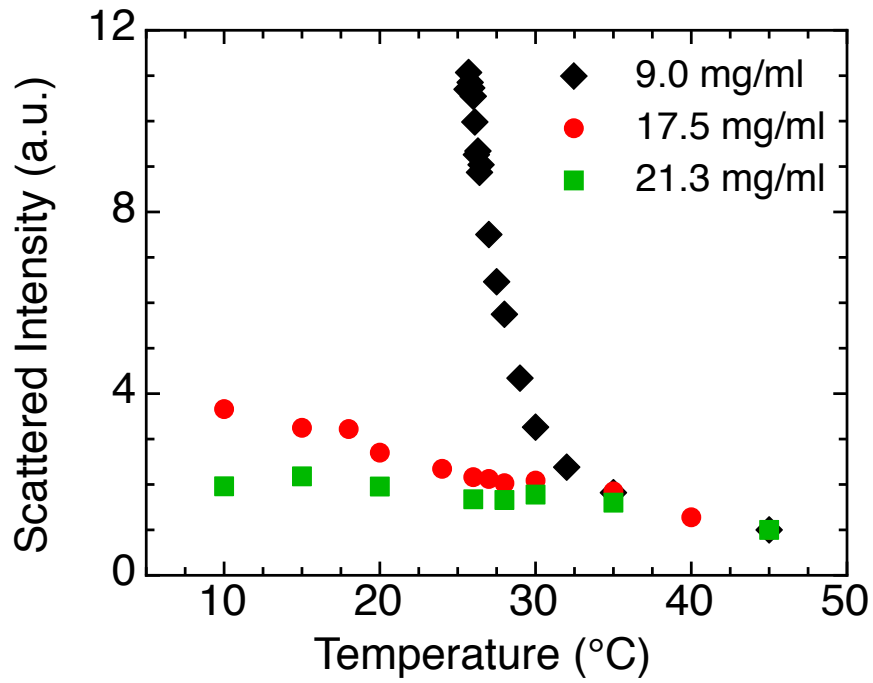


FIG. 2. Total scattered intensity as a function of  $T$  for DNA NS samples at three distinct concentrations:  $c_1 = 17.5 \text{ mg/ml}$  (red dots),  $c_2 = 21.3 \text{ mg/ml}$  (green squares),  $c^* = 9.0 \text{ mg/ml}$  (black diamonds). Data at the critical concentration  $c^*$  are taken from Ref. [23]

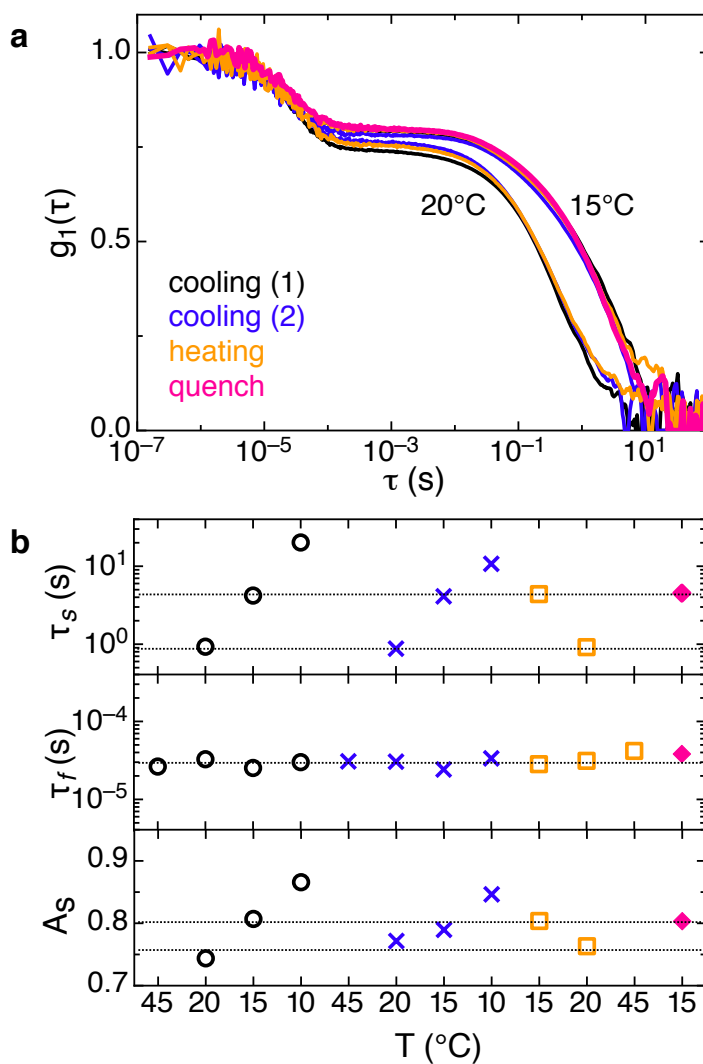


FIG. 3. (a) Intermediate scattering functions  $g_1(\tau)$  of the  $c_1$  sample measured at  $T = 15^\circ\text{C}$  and at  $T = 20^\circ\text{C}$  after various thermal histories: slowly cooling from  $45^\circ\text{C}$  (black lines), slowly cooling from  $45^\circ\text{C}$  after holding the sample for 6 months at  $4^\circ\text{C}$  (blue lines), slowly heating from  $10^\circ\text{C}$  (orange lines), fast cooling from  $45^\circ\text{C}$  (pink lines). (b) Fast and slow characteristic times and non-ergodicity factor determined from  $g_1(\tau)$  at the  $T$  sequentially adopted to thermalize the sample.

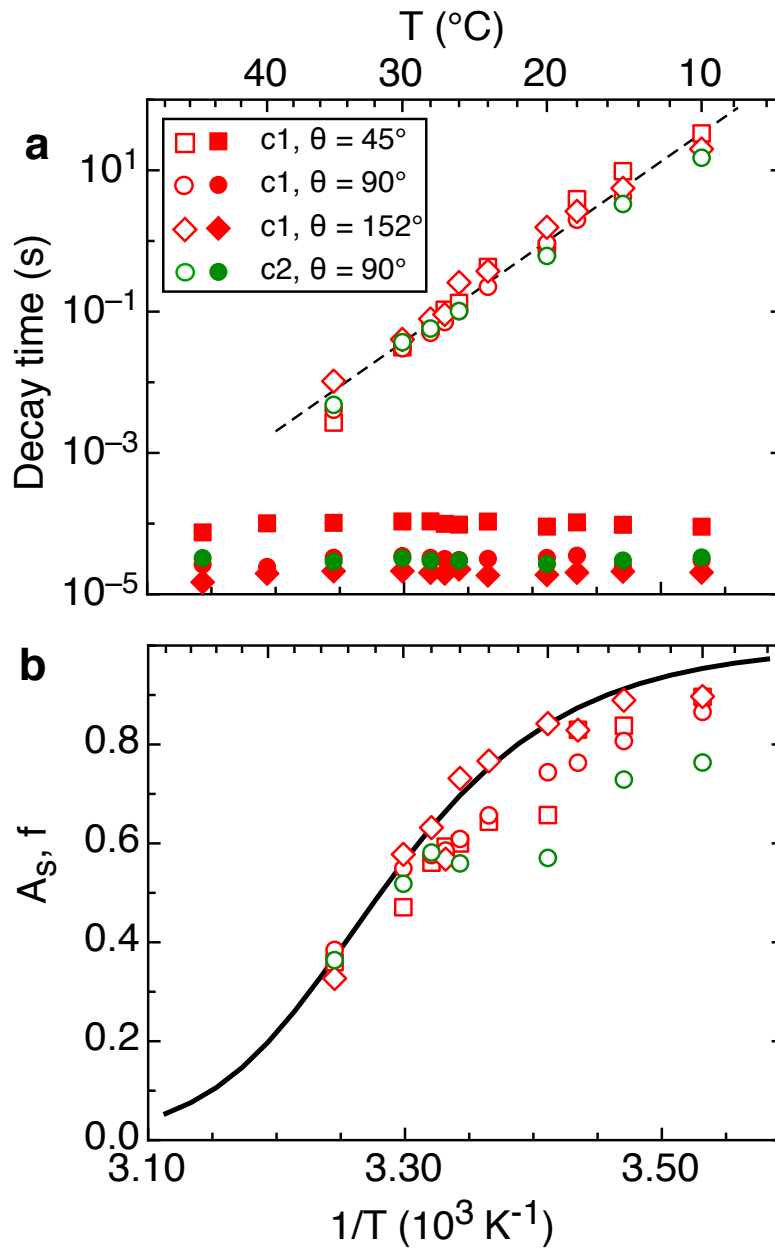


FIG. 4. (a) Dependence on  $1/T$  (bottom axis) and  $T$  (top axis) of the characteristic times  $\tau_f$  (full dots) and  $\tau_s$  (empty dots) measured at three scattering angles in the  $c_1$  sample (red symbols), and at  $90^\circ$  in the  $c_2$  sample (green symbols).  $\tau_f$  is constant with  $T$ , while  $\tau_s$  slows down of more than five order of magnitude. The dashed line shows the best fit to all the data of the Arrhenius law  $\ln(\tau_s)$  vs  $(RT)^{-1}$ . (b) Amplitude  $A_s$  of the slow relaxation process.  $A_s$  increases on cooling, growing upon lowering  $T$  to  $\approx 0.9$  ( $c_1$ ) and  $\approx 0.8$  ( $c_2$ ). The full black line indicates the fraction  $f$  of paired bases (thus ranging from 0 to 1) as calculated by NUPACK [38] for the sequence  $CGATCG$ , at the same concentration and ionic strength as in the experimental sample.

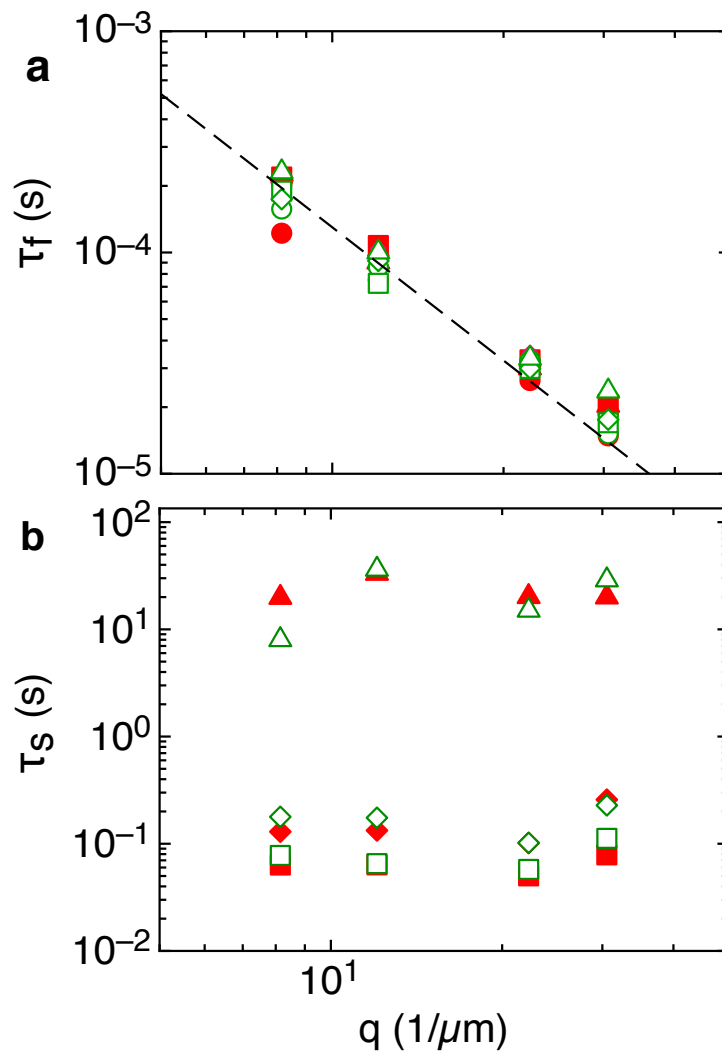


FIG. 5. Dependence on  $q$  of the characteristic times for  $\tau_f$  (pane a) and  $\tau_s$  (pane b) DNA-NS in the  $c_1$  sample (red symbols) and in the  $c_2$  sample (green symbols). Data are shown for  $T = 45^\circ\text{C}$  (dots),  $35^\circ\text{C}$  (squares),  $26^\circ\text{C}$  (diamonds),  $10^\circ\text{C}$  (triangles). The dashed line shows  $q^{-2}$  dependence, for comparison.  $\tau_f$  is found to be  $T$  independent and  $q$  dependent, while  $\tau_s$  is  $T$  dependent and  $q$  independent.